Quantitative evaluation of a mechanical simulator for power system stability

Yuko Omagari, and Tsuyoshi Funaki

Abstract—**Intuitively understanding the behavior of a power system is difficult because electricity is invisible. K. Noda proposed a mechanical simulator of a power system model to help understand power system behavior by representing it visually. The validity of the mechanical simulator was confirmed qualitatively. This study quantitatively evaluates the mechanical simulator through experiments that assess the accuracy of its analogy with the power system model. To this end, the steady-state and transient stability limit in the mechanical simulator are demonstrated. The limitation on the accuracy of the mechanical simulator is evaluated.**

Keywords: **mechanical simulator, power system, steady-state stability, transient stability.**

I. INTRODUCTION

A power system is a nonlinear dynamical system. Its main objective is to deliver electric energy to consumers. Stability of a power system significantly influences the reliability of its operation. Even smart grids cannot avoid stability problems, because their configuration is similar to that of conventional power systems [1]. For the successful operation of a power system, it is necessary to understand the phenomena arise in a power system involved with power system stability.

Traditionally, power system stability has been associated with generator rotor angle dynamics, which are described by a second-order differential equation (swing equation). Interconnected synchronous machines in a power system are required to operate in synchronism when subjected to disturbance and the ability to achieve this is called power system stability [2]. Physically, this requires balance between the mechanical power applied to each generator and its electrical power output. Any imbalance of power would accelerate or decelerate the machine rotor. If the difference in the rotor angle between any two machines increases indefinitely, that is, a generator loses synchronism with the rest of the system, the power system is unstable. Power system stability is analytically studied on the basis of the swing equation of the generator. However, intuitively understanding the power system behavior obtained by the stability study is difficult because electricity is invisible.

A mechanical simulator of a power system model may help intuitively understand power system behavior by representing it visually. For understanding power system stability, K. Noda proposed a mechanical simulator of a two-machine power system model, which consists of a rotating mass and spring [3]. It is easy to understand power system behavior, which refers to the acceleration/deceleration of a rotor angle, by representing a synchronous machine using a rotating mass. The validity of the mechanical simulator was qualitatively confirmed on the basis of the mathematical expressions of the mechanical simulator and the power system model [3]. Furthermore, the electric components in the power system model are represented by the mechanical components in the mechanical simulator. The quantitative evaluation of the mechanical simulator is required to assess the accuracy of the analogy of its behavior with that of the power system model [4]. This study quantitatively validates the mechanical simulator with the power system model through experiments and investigates the limitation on the accuracy of the mechanical simulator to represent power system behavior. To this end, the steady-state and transient stability limit of a power system in the mechanical simulator is demonstrated.

The rest of the paper is organized as follows. Section II describes a two-machine power system model and power system stability is studied on the basis of this model. Section III reviews the mechanical simulator of a two-machine power system model and discusses the analogy between the mechanical simulator and the power system model. The behavior of a power system in the mechanical simulator is also presented. Section IV provides the quantitative evaluation of the mechanical simulator through mechanical experiments. Finally, Section V presents the conclusions.

II. ELECTRIC POWER SYSTEM

A. Two-machine Power System Model

The simplest power system consists of a generator, a transmission line, and a load. Figure 1 shows a single-phase equivalent circuit of a two-machine power system. A synchronous generator and a synchronous motor are interconnected through a transmission line having a reactance X. $V_G \angle \delta$ and $V_M \angle 0$ are the phasor expressions of the internal voltages of the machines. This simplest system is useful in describing the basics of power system behavior. Power system stability is studied for the two-machine power system in Fig. 1.

B. Power System Stability

Interconnected synchronous machines in a power system are required to operate in synchronism when subjected to

Fig. 1.   Two-machine power system.

(a)   Power−angle relationship.

(b)   Energy-angle relationship.

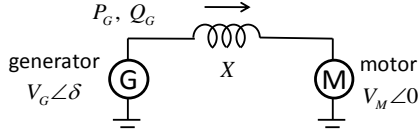Fig. 2.   Power-angle and energy-angle relationship of a single-machine infinite bus system.

disturbance, and the ability to achieve this is called power system stability. This stability is typically classified into steady-state and transient, depending on the severity of disturbance [2].

1)   Swing Equation

The dynamics of a synchronous generator are governed by the following second-order differential equation.

$$M \frac{d^2\delta}{dt^2} + D \frac{d\delta}{dt} = P_m - P_e \qquad (1)$$

Where, M is the inertia constant, δ is the rotor angular displacement with respect to the synchronously rotating reference, and D is the damping coefficient. P_m and P_e are the mechanical power input and the electrical power output of a generator, respectively. The imbalance between P_m and P_e accelerates or decelerates the rotor.

For the two-machine power system, the real and reactive powers at the generator are given as functions of phase angle δ.

$$P_G = \frac{V_G V_M}{X} \sin \delta, \quad Q_G = \frac{V_G^2 - V_G V_M \cos \delta}{X} \qquad (2)$$

P_G in (2) corresponds to P_e in (1). The power at the motor is equivalent to the transmitted power P_G from the generator. The power−angle characteristic in (2) gives nonlinearity in the power system operation.

2)   Steady-state Stability

Steady-state stability is the ability of a power system to maintain synchronism when subjected to small disturbance such as gradual change in load. The steady-state stability can be studied by linearizing (1) about an operating point [5]–[8].

For simplicity, the two-machine power system of Fig. 1 is integrated into one equivalent machine and infinite bus system [9]. Linearizing (1) for constant P_m and negligible damping effect, we get

$$M \frac{d^2\Delta\delta}{dt^2} = -\Delta P_e = -\frac{dP_e}{d\delta}(\Delta\delta), \qquad (3)$$

where Δ denotes a small deviation.

The characteristic equation of (3) has two roots:

$$\pm \sqrt{-\frac{1}{M} \cdot \frac{dP_e}{d\delta}} = \pm \sqrt{-\frac{1}{M} \cdot \frac{V_G V_M}{X} \cos \delta} \qquad (4)$$

The system is stable in the range of $\delta \leq 90°$: both roots are on the imaginary axis, where δ oscillation does not diverge. The system is unstable in the range of $\delta > 90°$: both roots are real, positive and negative, and δ results in divergence. At $\delta = 90°$, the system is at the stability limit. Thus, the steady-state stability power limit is given by

$$P_{max} = \frac{V_G V_M}{X}. \qquad (5)$$
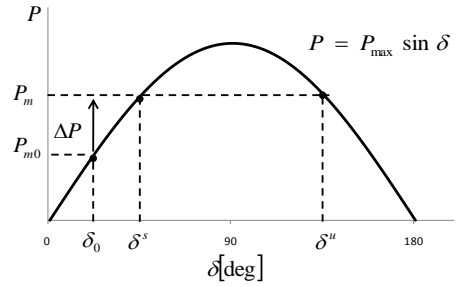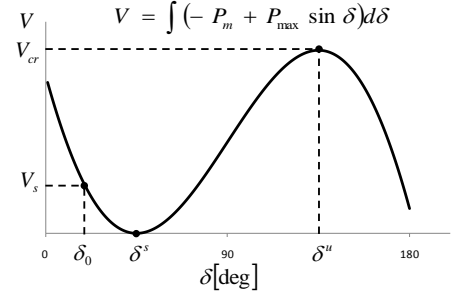
3)   Transient Stability

Transient stability is the ability of a power system to maintain synchronism when subjected to large disturbance, such as a short-circuit fault on a transmission line and loss of a large load. There are two commonly used methods for a transient stability study: time-domain simulation and energy function method. In the time-domain simulation method, (1) is solved numerically to discriminate whether the rotor angle increases indefinitely or oscillates about an equilibrium point. The energy function method is a special case of the Lyapunov's second method and is applied to the transient stability study as follows [10]–[15].

Recognizing that $P_e = P_{max} \sin \delta$, the energy function $V (\delta, \omega)$ of the system for (1) is defined as

$$V(\delta, \omega) = \frac{1}{2} M\omega^2 + \int_{\delta^s}^{\delta} (- P_m + P_{max} \sin \delta)d\delta, \qquad (6)$$

where $\omega = d\delta/dt$. Note that the damping component in (1) is neglected. The first term is kinetic energy and the second is potential energy, and δ^s is the post-disturbance stable equilibrium point. The critical energy V_{cr} at the stability boundary is equal to the system potential energy at the post-disturbance unstable equilibrium point δ^u.

The transient behavior of a single-machine infinite bus system is studied for local load shedding by using the energy function. Figure 2(a) shows the power–angle relationship of the system and the ordinate gives the transmitted power. Figure 2(b) shows the energy–angle relationship of the system. The electrical load P_L locally connected to the power station is included in the mechanical power input P_m : $P_m = P_m' - P_L$, where P_m' is the net mechanical power input from a prime mover. When the large local load ΔP, which is a part of $P_{L,}$ is

shed, there is surplus of mechanical power input over electrical power output [Fig. 2(a)]. Equilibrium points of the post-disturbance system are given for $d^2\delta/dt^2 = 0$ and $d\delta/dt = 0$, and the condition that two equilibrium points exist is considered as shown in Fig. 2(a). The post-disturbance stable δ^s and unstable δ^u equilibrium points are given by

$$\delta^s = \arcsin\left(\frac{P_m}{P_{\max}}\right), \quad \delta^u = \pi - \delta^s. \quad (7)$$

The initial conditions at the onset of the disturbance are $\omega = 0$ and $\delta = \delta_0$, where δ_0 is the operating point before the onset of disturbance. Then, the energy V_s of the system is

$$V_s = \int_{\delta^s}^{\delta_0} \left(- P_m + P_{\max} \sin \delta\right) d\delta. \quad (8)$$

On the other hand, the critical energy V_{cr} at the stability boundary of the system is

$$V_{cr} = \int_{\delta^s}^{\delta^u} \left(- P_m + P_{\max} \sin \delta\right) d\delta. \quad (9)$$

If V_s is less than V_{cr}, then the system is stable; if it is greater, then the system is unstable, that is, δ diverges and the generator falls out of step. At $V_s = V_{cr}$, the system is at the stability limit. Thus, the criterion for the stability is given by

$$\int_{\delta^s}^{\delta_0} \left(- P_m + P_{\max} \sin \delta\right) d\delta \leq \int_{\delta^s}^{\delta^u} \left(- P_m + P_{\max} \sin \delta\right) d\delta. \quad (10)$$

Substituting $P_m = P_{\max} \sin \delta^s$ and solving (10), we get

$$\cos \delta_0 - \cos(\pi - \delta^s) = (\pi - \delta^s - \delta_0) \sin \delta^s. \quad (11)$$

Because δ^s cannot be expressed in the closed form, it must be calculated numerically using an iterative convergence calculation. The maximum local load shedding $\Delta P_{\max}$ is given by
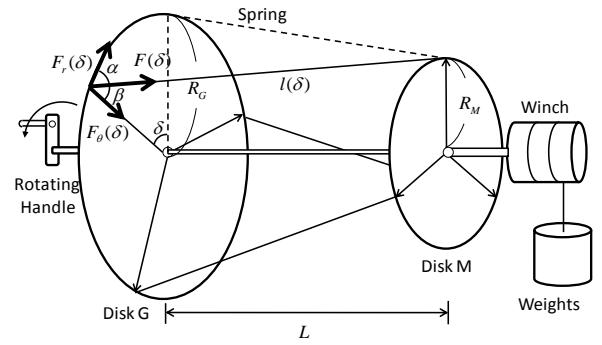
$$\Delta P_{\max} = P_{\max} \sin \delta^s - P_{m0}. \quad (12)$$

III. MECHANICAL SIMULATOR OF POWER SYSTEM MODEL

This section reviews the mechanical simulator of the two-machine power system model. The qualitative validation of the mechanical simulator is derived on the basis of the correspondence in the mathematical expressions of the mechanical simulator and the power system model. Then, the behavior of the power system in the mechanical simulator is illustrated.

A. Mechanical Simulator of Two-machine Power System Model

Figure 3(a) shows the schematic diagram of the mechanical simulator of the two-machine power system model developed by K. Noda [3]. Rotating disks G and M represent the generator and motor, respectively. They pivot independently on a common axis and are interconnected by three springs. The three springs are equiangularly placed on the fringe of the disks to represent a balanced three-phase system. The rotating handle and weights represent mechanical power input and output of the generator and motor, respectively. The image of the mechanical simulator constructed in this study is shown in Fig. 3(b).

(a)   Schematic diagram of mechanical simulator.

(b)   Image of mechanical simulator.

Fig. 3.   Mechanical simulator of two-machine power system model.

B. Analogy of Mechanical Simulator with Power System Model

The dynamics of the disk are governed by the following second-order differential equation.

$$J \frac{d^2\delta}{dt^2} + \mu = T_m - T_e \quad (13)$$

Where, J is the moment of inertia of the disk and T_m and T_e are the torques acting on the disk originating from the rotating handle or weights and from the spring tension, respectively. μ is the dynamic friction torque and δ is the displacement angle between the two disks. Note that the damping component μ is assumed to be constant for the slow rotation of the disk. By comparing (13) with (1), correspondence between parameters and variables are found. While (13) is given in a stationary reference frame, (1) is given in a rotating reference frame. The mechanical simulator at the stationary state corresponds to the power system model at a synchronous speed where the imbalance between P_m and P_e is zero.

Furthermore, the mechanical simulator shows correspondence with the power system model in the algebraic equations. The spring length is expressed as a function of δ.

$$l(\delta) = \sqrt{L^2 + (R_M \sin \delta)^2 + (R_G - R_M \cos \delta)^2} \quad (14)$$

Where, R_G and R_M are radii of disks G and M, respectively, and L is the distance between the two disks.

The spring tension $F(\delta)$ of a linear spring is given by

$$F(\delta) = k(l(\delta) - l_0), \quad (15)$$

where k is a spring constant and l_0 is the natural length of the

spring. When $F(\delta)$ is proportional to the spring length, it is given by

$$F(\delta) = F(0°) \cdot \frac{l(\delta)}{l(0°)} = \frac{l(\delta)}{D} , \qquad (16)$$

where $D \equiv l(0°)/F(0°)$.

$F(\delta)$ acting on disk G can be decomposed into tangential $F_r(\delta)$ and centripetal $F_\theta(\delta)$ components.

$$F_r(\delta) = F(\delta) \cdot \cos \alpha, \quad F_\theta(\delta) = F(\delta) \cdot \cos \beta \qquad (17)$$

Where, α is the angle between $F(\delta)$ and $F_r(\delta)$ and β is the angle between $F(\delta)$ and $F_\theta(\delta)$. $\cos\alpha$ and $\cos\beta$ are given by

$$\cos \alpha = \frac{R_M \sin \delta}{l(\delta)} , \quad \cos \beta = \frac{R_G - R_M \cos \delta}{l(\delta)} . \qquad (18)$$

Substituting (16) and (18) into (17), we get

$$F_r(\delta) = \frac{R_M \sin \delta}{D} ,$$

$$F_\theta(\delta) = \frac{R_G - R_M \cos \delta}{D} . \qquad (19)$$

The product of the tangential force $F_r(\delta)$ and the radius R_G gives the torque $T_r(\delta)$ acting on disk G. Similarly, the product of the centripetal force $F_\theta(\delta)$ and R_G gives the imaginary torque $T_\theta(\delta)$.

$$T_r(\delta) = F_r(\delta) \cdot R_G = \frac{R_G R_M \sin \delta}{D} ,$$

$$T_\theta(\delta) = F_\theta(\delta) \cdot R_G = \frac{R_G^2 - R_G R_M \cos \delta}{D} \qquad (20)$$

Comparing (20) with (2), the following correspondence exists between the parameters and variables in the mechanical simulator and the power system model:

- Radii R_G and R_M correspond to voltages V_G and V_M, respectively. The distance from the common axis to the spring corresponds to the voltage at the corresponding point on a transmission line.
- The product of the tangential component of spring tension $F_r(\delta)$ and radius R_G gives torque $T_r(\delta)$, which corresponds to real power P_G.
- The product of the centripetal component of spring tension $F_\theta(\delta)$ and radius R_G gives imaginary torque $T_\theta(\delta)$, which corresponds to reactive power Q_G.
- The reciprocal of spring tension D [$\equiv l(0°)/F(0°)$] corresponds to transmission line reactance X.

Thus, the analogy between the mechanical simulator and the power system model is clear based on the correspondence of their differential and algebraic equations.

The mechanical–mathematical model analogy proposed by K. Noda was described in (14)–(20) [16]. This strict analogy is established under the condition that the spring tension is proportional to the spring length with $l_0 = 0$. In this case, $T_r(\delta)$ and $T_\theta(\delta)$ are given by (20) where $D = l(0°)/F(0°)$.
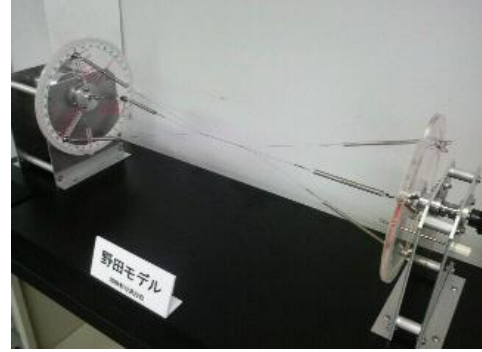
However, the spring tension is generally not proportional to the spring length with $l_0 > 0$. In this case, $F_r(\delta)$ in (19) is rewritten as

$$F_r(\delta) = \frac{R_M \sin \delta}{l(\delta)/F(\delta)} . \qquad (21)$$

Then, $T_r(\delta)$ in (20) is rewritten as
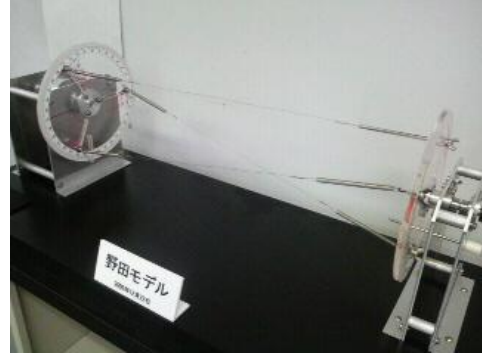
(a) Steady-state stability limit of a power system in mechanical simulator.

(b) Out of step synchronous generator in mechanical simulator.
Fig. 4. Behavior of a two-machine power system model in mechanical simulator.

$$T_r(\delta) = F_r(\delta) \cdot R_G = \frac{R_G R_M \sin \delta}{l(\delta)/F(\delta)} . \qquad (22)$$

$T_\theta(\delta)$ is obtained similarly. Comparing (22) with (2), it is found that $l(\delta)/F(\delta)$, which varies with δ, corresponds to transmission line reactance X. Thus, when the spring tension is non-proportional to the spring length, the analogy between the mechanical simulator and the power system model is not strict, but approximate.

C. Behavior of a Power System in the Mechanical Simulator

Because the mechanical simulator is analogous to the power system model in the expressions of the differential and algebraic equations, it simulates the power system behavior obtained in Section II.B.

The behavior of a power system subjected to small disturbance is simulated in the mechanical simulator as follows. As weight is added in small increments, torque T_r increases and disk M rotates with δ gradually increasing from 0°. Interpreted in terms of a power system, this change occurs according to increase in the load, and then the amount of transmitted power and the phase angle between the internal voltages of the generator and motor increase. T_r reaches its maximum value at $\delta = 90°$ [Fig. 4(a)]. As more weight is added, δ increases but T_r decreases, and the torque due to the weight acting on disk M will not balance T_r. Then, disk M is accelerated and δ increases indefinitely, resulting in three springs intersecting at the midpoint [Fig. 4(b)]. Thus, the corresponding power system is considered unstable. This

TABLE I
MECHANICAL AND NUMERICAL EXPERIMENTS RESULTS

		mechanical simulator [pu[*1]]	power system model with X_{ref} [pu[*2]]	power system model with $X(\delta)$ [pu[*3]]
steady-state stability power limit		1.81 (δ^l=85°)	1.74 (δ^l=90°)	1.76 (δ^l=90°)
maximum local load shedding	δ_0=20.0°	0.88 (δ^e=59°)	0.82 (δ^e=56°)	0.85 (δ^e=57°)
	δ_0=40.0°	0.58 (δ^e=72°)	0.45 (δ^e=65°)	0.50 (δ^e=67°)
	δ_0=60.0°	0.27 (δ^e=83°)	0.17 (δ^e=75°)	0.21 (δ^e=79°)

[*1] [pu] = 1×10^{-2} [N·m], δ^l is the stability limit and δ^e is the equilibrium point
System base = 100 [MVA], Voltage base = 500 [kV], $V_G = V_M = 1$ [pu]
[*2] $X = 0.590$ [pu], [*3] $M = 7.63$ [MJ/rad] and $D = 2.99$

behavior of the power system in the mechanical simulator shows that the steady-state stability limit occurs at $\delta = 90°$ and the generator falls out of step at $\delta > 90°$. The maximum torque obtained in this manner corresponds to the steady-state stability power limit of a power system.

The mechanical simulator is also used to simulate the transient behavior of a single-machine infinite bus system following local load shedding. When the mechanical simulator is used for this purpose, disk G is stuck so as to not rotate and represent an infinite bus. Disk M and the weights represent a generator and its mechanical power input, respectively. An abrupt change in P_m of a generator is simulated by suddenly adding a large weight ΔW. Disk M begins to accelerate because of ΔW. If ΔW is small, disk M rotates and stops at a new equilibrium point, and the corresponding power system is considered stable. On the other hand, if ΔW is very large, disk M is accelerated and δ increases indefinitely, resulting in the three springs intersecting at the midpoint. Then, the corresponding power system is considered unstable. The maximum increase in torque obtained in this manner corresponds to the maximum local load shedding of a power system.

IV. RESULTS AND DISCUSSION

This section quantitatively evaluates the mechanical simulator with the power system model by a comparative study on the steady-state stability power limit and the maximum local load shedding.

The strict analogy between the mechanical simulator and the power system model is established when the proportionality of the spring tension to the spring length is satisfied. However, the mechanical simulator has an intrinsic problem, that is, the non-proportional relationship between the spring tension and the spring length. Therefore, the behavior of the mechanical simulator is explained by compensating the non-proportionality of the spring tension to the spring length. In particular, it is evaluated by varying the transmission line reactance with δ in the power system model. The inherent limitation on the accuracy of the mechanical simulator due to the springs is evaluated.
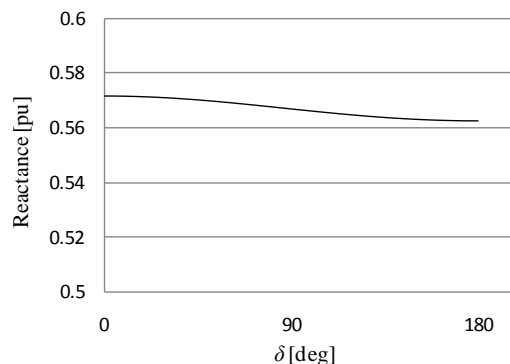

Fig. 5. Variation in transmission line reactance with δ.

A. Experiment Results

1) Mechanical Experiment Results

The physical parameters of the mechanical simulator are radius $R_G = R_M = 7.30 \times 10^{-2}$ [m] and distance $L = 4.90 \times 10^{-1}$ [m]. The relationship between spring tension F [N] and spring length $l(\delta)$ [m] is measured as $F = 4.55 \times l(\delta) - 0.671$. The springs are chosen so that they will not be stretched beyond their elastic limit when weights are added. The dynamic friction torque μ is evaluated to be 2.99×10^{-4} [N·m] by measuring the decay of the rotating speed of the freewheeling rotation of the disk. The maximum static friction torque of the disk is measured to be 1.29×10^{-3} [N·m] at which the disk with the stick condition starts to rotate.

The steady-state stability power limit and the maximum local load shedding in the mechanical simulator are experimentally obtained as in Section III.C. The maximum local load shedding are conducted for different initial conditions δ_0 of 20.0°, 40.0°, and 60.0° in the mechanical experiment. The results are shown in Table I. The corresponding δ^l and δ^e in the mechanical simulator are simultaneously shown in Table I.

2) Numerical Experiment Results

The parameters of the power system model are set to be equivalent to the physical parameters of the mechanical simulator.

The steady-state stability power limit and the maximum local load shedding in the power system model are obtained as
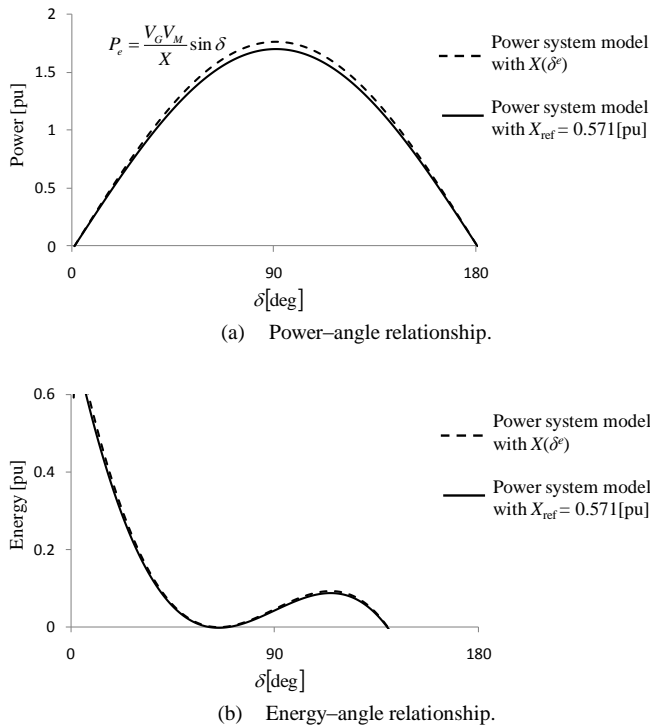
(a)   Power–angle relationship.

(b)   Energy–angle relationship.

Fig. 6.   Power–angle and energy–angle relationship of the power system model (For example, $\delta^e = 65°$ and $X(65°) = 0.569$ [pu]).

in Section II.B. The maximum local load shedding is evaluated with the energy function method for different initial conditions δ_0 of 20.0°, 40.0°, and 60.0°. The Newton–Raphson method is used to solve (11).

Numerical experiments are also performed on the power system model considering the non-proportionality of the spring tension to the spring length, that is, by varying transmission line reactance with δ. The equivalent transmission line reactance $X(\delta)$ is shown in Fig. 5. The maximum local load shedding is evaluated with the time-domain analysis for respective δ_0. Equation (1) is solved by the fourth-order Runge–Kutta method with a time step of 0.01 sec. The summarized results including the corresponding δ^l and δ^e in the power system model are simultaneously shown in Table I.

B. Discussion

1)   Steady-state Stability

The mechanical simulator provides a higher steady-state stability power limit than the power system model. The error of the mechanical simulator to the power system model is 4.02 [%]. In this study, an error within five percent is acceptable, due to the accuracy of the identified parameters of the mechanical simulator. Because the error is smaller than this criterion, it is quantitatively validated.

When the non-proportionality of the spring tension to the spring length is compensated, the error reduces to 2.84 [%]. This is explained as follows. In the numerical experiment, the steady-state stability power limit is calculated for the power system model with a transmission line reactance of $X_{ref} = 0.571$ [pu]. When the non-proportionality of the spring tension to the

spring length is compensated, the steady-state stability power limit at $\delta^l = 90°$ corresponds to that with $X(90°) = 0.567$ [pu] which is higher than that with $X_{ref} = 0.571$ [pu]. When the variation in the transmission line reactance with δ is considered in the power system model, the error of the mechanical simulator reduces.

The mechanical simulator validly represents the steady-state stability power limit in a power system. The influence of the non-proportionality of the spring tension to the spring length does not limit the accuracy of the mechanical simulator for the steady-state stability power limit.

2)   Transient Stability

The mechanical simulator provides higher maximum local load shedding than the power system model. The error of the mechanical simulator for the initial condition of $\delta_0 = 20.0°$, 40.0°, and 60.0° are 7.3, 29, and 59 [%], respectively. Because the error is larger than the criterion, it is not quantitatively validated.

The error of the mechanical simulator can be attributed to the non-proportionality of the spring tension to the spring length. Its influence on the maximum local load shedding is explained as follows. In the numerical experiment, the maximum local load shedding is calculated for the constant transmission line reactance X_{ref}. When the non-proportionality of the spring tension to the spring length is compensated, the equivalent transmission line reactance at the post-disturbance equilibrium point $\delta^e = 56°$, 65°, and 75° are 0.570, 0.569, and 0.568 [pu], respectively, which are smaller than X_{ref}. Figure 6 shows the power–angle and energy–angle relationships of the power system model with X_{ref} and $X(\delta^e)$. From Fig. 6(a), the maximum power in the power system model with $X(\delta^e)$ is higher than that of the power system model with X_{ref}. This increases the maximum transmittable power and enhances the transient stability of a power system. The critical energy of the power system model with X_{ref} for $\delta_0 = 20.0°$, 40.0°, and 60.0° are 0.234, 0.0898, and 0.0201 [pu], respectively. The corresponding critical energy of the power system model with $X(\delta^e)$ are 0.243, 0.0932, and 0.0209 [pu], respectively. Because the critical energy of the power system model with $X(\delta^e)$ is higher than that with X_{ref}, the maximum local load shedding in the model with $X(\delta^e)$ is higher. Therefore, although the dynamic variation in $X(\delta)$ is not considered in the above discussion, the mechanical simulator with the non-proportional spring is expected to provide higher maximum local load shedding than the power system model with X_{ref}. It should be noted that the error in the mechanical simulator is also attributed to the dynamic friction torque, which is not considered in the numerical experiment of the energy function analysis. This results in higher maximum local load shedding in the mechanical simulator than the power system model.

When the non-proportionality of the spring tension to the spring length is compensated, the error in the maximum local load shedding for $\delta_0 = 20.0°$, 40.0°, and 60.0° reduces to 3.5, 16, and 29 [%], respectively. However, a large error remains for a large δ_0. This may be attributed to the static friction

torque in the mechanical simulator that induces the hysteresis stick and slip behavior in the motion. The influence of the friction on the behavior of the mechanical simulator is difficult to evaluate and the static friction torque is not considered in the mechanical simulator equation and in the discussion of the analogy. The ratio of the dissipated energy resulting from the static friction torque to the elastic energy stored in the spring at δ^{u} may be high at a large δ_0. Therefore, the error in the mechanical simulator due to the static friction torque is high at a large δ_0. The error in the mechanical simulator for $\delta_0 = 20.0°$ is smaller than the criterion and the mechanical simulator is quantitatively validated for a small δ_0.

When the non-proportional relationship between spring tension and spring length is compensated, the mechanical simulator validly represents the maximum local load shedding in a power system at a small δ_0. However, the error in the mechanical simulator occurs due to the friction torque in the simulator.

V. Conclusions

Because electricity is invisible, it is difficult to intuitively understand the power system behavior obtained from a stability study. In this study, we described the mechanical simulator of a power system model, which provides a means of visualizing power system behavior. The qualitative analogy between the mechanical simulator and the power system model was derived, on the basis of the correspondence in their mathematical expressions. The strict analogy is established when the proportionality of the spring tension to the spring length is satisfied. The mechanical simulator has an intrinsic problem, that is, the non-proportional relationship between the spring tension and the spring length.

This study performed a quantitative evaluation of the mechanical simulator by comparing the mechanical experiment results with the numerical experiment results of the power system model. The validity of the mechanical simulator was quantitatively confirmed for the steady-state stability power limit. The error in the mechanical simulator reduced by compensating the non-proportionality between the spring tension and the spring length. The non-ideal characteristics of the spring did not limit the simulation of the steady-state stability power limit. When the non-proportionality of the spring tension to the spring length was compensated, the mechanical simulator was quantitatively validated with respect to the maximum local load shedding for the initial condition of a small phase displacement angle.

The error in the mechanical simulator is due to springs that have a non-proportional relationship between their tension and length. However, when this non-ideal characteristic of the spring is considered, the mechanical simulator validly represents power system behavior. The mechanical simulator can be used to aid in intuitively understanding power system behavior and the concept of power system stability.

The influence of springs can be eliminated by using springs that are proportional in tension and length. These details are covered in another paper. The error of the mechanical simulator to the power system model is expected to reduce for such springs.

VII. References

[1] Y.H. Song and A.T Johns ed., *Flexible ac transmission systems (FACTS)*, London: the Institution of Electrical Engineers, 1999.

[2] P. Kundur, *Power system stability and control*, New York: McGraw-Hill, 1994.

[3] K. Noda, " Kouryudenryokusouden no genri wo setsumeisuru kikaiteki rittaimokei," in *Proc. the 1973 Annual Meeting of IEEJ*, p. 1205, 1973 (in Japanese).

[4] Y. Omagari, and T. Funaki, "Experimental validation of an equivalent mechanical model for understanding power system stability," *ELEX*, vol. 7, no. 20, pp. 1578-1583, Oct. 2010.

[5] E. Clarke, "Steady-state stability in transmission systems calculation by means of equivalent circuits or circle diagrams," *AIEE Trans.*, vol. 45, pp. 22-41, Jan. 1926.

[6] N. Martins, "Efficient eigenvalue and frequency response methods applied to power system small-signal stability studies," *IEEE Trans. Power syst.*, vol. 1, no. 1, pp. 217-224, Feb. 1986.

[7] D.Y. Wong, G.J. Rogers, B. Porretta, and P. Kundur, " Eigenvalue analysis of very large power systems," *IEEE Trans. Power syst.*, vol. 3, no. 2, pp. 472-480, May. 1988.

[8] N. Uchida, and T. Nagao, "A new eigen-analysis method of steady-state stability studies for large power systems: S matrix method," *IEEE Trans. Power syst.*, vol. 3, no. 2, pp. 706-714, May. 1988.

[9] B.M. Weedy, *Electric power systems*, the second edition, New York: Wiley, 1972.

[10] P.C. Magnusson, "The transient energy method of calculating stability," *AIEE Trans.*, vol. 66, no. 1, pp. 747-755, 1947.

[11] P.D. Aylett, "The energy integral-criterion of transient stability limits of power systems," in *Proc. IEE*, vol. 105c, no. 8, pp. 527-536, Sep. 1958.

[12] G.E. Gless, "Direct method of Lyapunov applied to transient power system stability," *IEEE Trans.*, vol. PAS-85, no. 2, pp. 159-168, Feb. 1966.

[13] T. Athay, R. Podmore, and S. Virmani, "A practical method for the direct analysis of transient stability," *IEEE Trans.*, vol. PAS-98, no. 2, pp. 573-584, Mar./Apr. 1979.

[14] A.A. Fouad, V. Vittal, and Taekyoo Oh, "Critical energy for transient stability assessment of a multimachine power system," *IEEE Trans.*, vol. PAS-103, pp. 2199-2206, 1984.

[15] H.D. Chiang, F.F. Wu, and P.P. Varaiya, "Foundations of the potential energy boundary surface method for power system transient stability analysis," *IEEE Trans.*, vol. CAS-35, pp. 712-728, Jun. 1988.

[16] K. Noda ed., *Power control and information series dai ikkan denryoku keitou no seigyo*, Tokyo: Denkishoin, 1986 (in Japanese).